Hydrogen Absorption and Desorption by the Li−Al−N−H System

Yoshitsugu Kojima,*,† Mitsuru Matsumoto,† Yasuaki Kawai,† Tetsuya Haga,† Nobuko Ohba,† Kazutoshi Miwa,† Shin-ichi Towata,† Yuko Nakamori,‡ and Shin-ichi Orimo‡

Toyota Central R&D Labs, Inc., Nagakute-cho, Aichi-gun, Aichi, 480-1192, Japan, and Institute for Materials Research, Tohoku University, Sendai 980-8577, Japan

Received: January 24, 2006; In Final Form: March 28, 2006

Lithium hexahydridoaluminate Li_3AlH_6 and lithium amide $LiNH_2$ with 1:2 molar ratio were mechanically milled, yielding a Li−Al−N−H system. $LiNH_2$ destabilized Li_3AlH_6 during the dehydrogenation process of Li_3AlH_6, because the dehydrogenation starting temperature of the Li−Al−N−H system was lower than that of Li_3AlH_6. Temperature-programmed desorption scans of the Li−Al−N−H system indicated that a large amount of hydrogen (6.9 wt %) can be released between 370 and 773 K. After initial H_2 desorption, the H_2 absorption and the desorption capacities of the Li−Al−N−H system with a nano-Ni catalyst exhibited 3−4 wt % at 10−0.004 MPa and 473−573 K, while the capacities of the system without the catalyst were 1−2 wt %. The remarkably increased capacity was due to the fact that the kinetics was improved by addition of the nano-Ni catalyst.

1. Introduction

H_2 can be stored in tanks as compressed[1] or liquefied H_2[1] or by adsorption on carbon materials.[1−3] It can also be stored in H_2-absorbing alloys (metal hydrides), metal hydrides with high dissociation pressure,[4] or as a chemical hydride, such as $NaBH_4$,[5−7] $LiBH_4$,[8,9] $NaAlH_4$,[10,11] or MgH_2,[12−14] as well as in an organic hydride, such as methylcyclohexane or Decalin.[15] In recent years, attention has been given to metal nitrides,[16−21] after Chen et al. had reported that metal nitride (Li_3N) absorbed and desorbed hydrogen at high temperature (468−528 K).[16] It has been reported that the partial substitution of lithium by magnesium in the nitride/imide system (Li−Mg−N−H) destabilizes the Li−N−H system.[17−21] For useable H_2 storage, H_2 absorption/desorption at ambient temperature is necessary. Recently, it has been shown that the dehydriding reaction of the mixtures of $LiAlH_4$ and $LiNH_2$ ($LiAlH_4/2LiNH_2$, $LiAlH_4/LiNH_2$) can occur at room temperature during mechanical milling.[22,23] Hydrogen (6 wt %) was released from $LiAlH_4/LiNH_2$ after 10 h ball milling.[23] Fang et al. investigated dehydrogenation properties of the mixture of $LiAlH_4$ and $LiNH_2$ ($2LiAlH_4/LiNH_2$).[24] Thermogravimetric analysis indicated that a large amount of hydrogen (∼8.1 wt %) can be released between 358 and 593 K.[24] Accordingly, $LiNH_2$ effectively destabilized $LiAlH_4$. However, little information has emerged on the reversibility of those hydrogen capacities.

In this work, attention was given to Li_3AlH_6 having reversible H_2 storage, while $LiAlH_4$ presents irreversible H_2 storage.[25] We present, for the first time, that hydrogen can be reversibly stored by the mixture of Li_3AlH_6 and $LiNH_2$ (Li−Al−N−H system) at a pressure of 10−0.004 MPa and 473−573 K.

2. Experimental Section

Lithium aluminum hydride (lithium tetrahydridoaluminate $LiAlH_4$, Wako Pure Chemical Industries, Ltd., Japan; molecular weight, 37.95; density, 0.92 g/cm^3), lithium hydride LiH (Sigma-Aldrich; molecular weight, 7.95; density, 0.82 g/cm^3; purity, 95%), and lithium amide $LiNH_2$ (Alfa Aesar; molecular weight, 22.96; density, 1.18 g/cm^3) were used in this experiment. Lithium hexahydridoaluminate Li_3AlH_6 was prepared by ball-milling a stoichiometric mixture of LiH and $LiAlH_4$ (taken in 1:2 molar ratio) in an Ar atmosphere for 24 h. [26] The nano-Ni catalyst with the diameter of about 20 nm was purchased from Shinku-Yakin. High-purity H_2 gas (>99.99999%) was used as a reaction atmosphere. Mechanical milling was performed in a planetary ball mill (Fritsch P-5) to prepare Li−Al−N−H systems. The mill container (Cr−Mo steel pot with an internal volume of 300 mL) was loaded with about 5 g of Li_3AlH_6 and $LiNH_2$ powders with 1:2 molar ratio and 40 pieces of steel ball with a diameter of 9.5 mm (ball-to-powder mass ratio of 28:1). Li_3AlH_6 and $LiNH_2$ were milled at 400 rpm of rotational speed and 200 rpm of revolutional speed for 24 h in an Ar gas atmosphere at a pressure of 0.1 MPa and room temperature (296 K), yielding a Li−Al−N−H system. To clarify the catalytic effect on the H_2 absorption and desorption properties, a small amount of nano-Ni (5 wt %) was added to the powders of Li_3AlH_6 and $LiNH_2$, and then, these were mechanically milled under the same conditions used to prepare the Li−Al−N−H system without the catalyst.

ThermoNicolet AVATAR 360 E.S.P. FT-IR spectrometer with ATR system was used for IR studies in an inert atmosphere of N_2. X-ray diffraction (XRD) intensity curves in an inert atmosphere (Ar) were recorded with Cu Kα radiation (50 kV, 300 mA) filtered by a monochromator using Rigaku Rint-TTR. The apertures of the first, second, and third slits were 0.5, 0.5, and 0.15 mm, respectively. It is noted that the amorphous-like background in the XRD curves is attributed to thin polymer films that were used for shielding from aerial O_2 and H_2O. With a specially designed apparatus, temperature-programmed desorption (TPD) scans were carried out at a heating rate of 2 K/min in an Ar flow of 85 mL/min. The decomposed hydrogen H_2 and ammonia NH_3 were released from the specimen and were monitored by two gas chromatographs with an automatic

* Corresponding author. Tel: +81-561-63-5325. Fax: +81-561-63-6137. E-mail: kojima@mosk.tytlabs.co.jp.
† Toyota Central R&D Labs, Inc.
‡ Tohoku University.

10.1021/jp060525z CCC: $33.50
Published on Web 04/21/2006

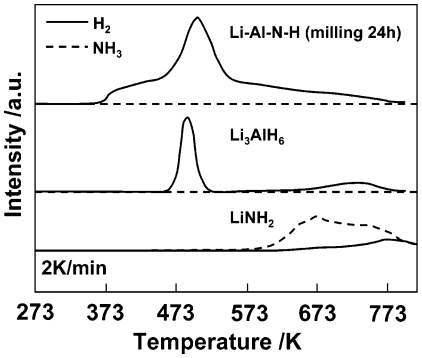

Figure 1. TPD spectra for Li−Al−N−H system ($Li_3AlH_6/2LiNH_2$), Li_3AlH_6, and $LiNH_2$.

gas sampler, digital integrators, and thermal conductivity detectors. Activated charcoal (60−80 mesh, carrier gas Ar, 40 mL/min) and Porapak N (80−100 mesh, carrier gas He, 40 mL/min) columns from Shimadzu GLC Ltd. were used to separate H_2 and NH_3. H_2 absorption and desorption isotherms were measured with a pressure-composition-temperature (PCT) automatic measuring system (Sievert's type apparatus, maximum pressure: 10 MPa) provided by Suzuki Shokan Co. Ltd., Japan.

First-principles calculations were performed to investigate the heat of formation of the Li−Al−N−H system by the ultrasoft pseudopotential method based on the density functional theory. The generalized gradient approximation formula was applied to the exchange-correlation energy. The effects of the zero-point energy were not taken into consideration. The details of computational procedure can be found in refs 27 and 28.

3. Results and Discussion

Figure 1 compares TPD spectra of H_2 from the Li−Al−N−H system ($Li_3AlH_6/2LiNH_2$) mixed by mechanical milling for 24 h. One desorption peak and one shoulder are observed at 500 K and around 380 K in the Li−Al−N−H system without any catalysts. The profiles of Li_3AlH_6 and $LiNH_2$ are also shown as references. The dehydrogenation starting temperature of the Li−Al−N−H system is 370 K. This value is close to those for the ball-milled mixtures of $LiAlH_4$ and $LiNH_2$ [$LiAlH_4/2LiNH_2$ (373 K)[22], $2LiAlH_4/LiNH_2$ (358 K)[24]] and lower than those of Li_3AlH_6 (460 K, Figure 1) and a conventional Li−N−H system [$2LiH/LiNH_2$ (493 K),[24] $LiH/LiNH_2$ (453 K)[29]]. We found that $LiNH_2$ destabilizes Li_3AlH_6.

Li_3AlH_6 has two desorption peaks at 487 and 730 K, as shown in Figure 1. The desorption peaks at 487 and 730 K correspond to the dehydriding reaction of the two-step reaction of eq 1[22,26,30]

$$Li_3AlH_6 \rightarrow 3LiH + Al + {}^3/_2H_2 \rightarrow LiAl + 2LiH + 2H_2 \quad (1)$$

The desorption peak at 500 K of the Li−Al−N−H system is similar to that of Li_3AlH_6 (487 K). It is suggested that the Li−Al−N−H system includes LiH and Al after the thermal desorption reaction below decomposition temperature of LiH (673 K). The H_2 desorption capacity of the Li−Al−N−H system estimated from the peak area of TPD spectrum (Figure 1) is 6.9 wt %, being comparable to the value of Li_3AlH_6 (experimental value, 7.3 wt %; theoretical value, 7.5 wt %). The TPD spectra of NH_3 and H_2 from pure $LiNH_2$ were examined in this work, as shown in Figure 1. NH_3 is drastically desorbed starting at 573 K. Above 623 K, the desorption reaction of H_2 occurs due to the decomposition of NH_3. Here, NH_3 was not detected from the Li−Al−N−H system.

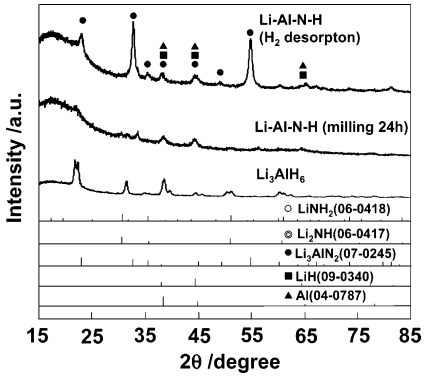

Figure 2. X-ray diffraction intensity curve for Li−Al−N−H system together with the data of Li_3AlH_6, $LiNH_2$ (JCPDS file no. 06-0418), Li_2NH (JCPDS file no. 06-0417), Li_3AlN_2 (JCPDS file no. 07-0245), LiH (JCPDS file no. 09-0340), and Al (JCPDS file no. 04-0787).

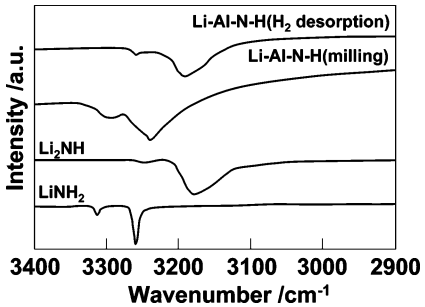

Figure 3. IR absorption spectra of Li−Al−N−H system together with the data of Li_2NH[31,32] and $LiNH_2$.[31,32]

Figure 2 shows the XRD curves of the Li−Al−N−H system together with the data of Li_3AlH_6, $LiNH_2$,[31] Li_2NH,[31] Li_3AlN_2,[31] LiH,[31] and Al.[31] The Li−Al−N−H system shows broad and small diffraction peaks. These peaks establish the small size of the crystallites and/or lattice distortions. After the thermal desorption reaction of H_2, we notice that the diffraction peaks of the Li−Al−N−H system at 2θ of 23.0°, 32.8°, 35.4°, 37.9°, 45.0°, 49.3°, and 54.7° are raised from (211), (322), (321), (400), (332), (431), and (440) planes of Li_3AlN_2. The XRD peaks of the Li−Al−N−H system at 2θ of 38−39°, 44−45°, and 64−65° comes from LiH and Al. LiH and Al peaks overlap on the XRD curves.

The infrared spectra of the Li−Al−N−H system, Li_2NH,[32,33] and $LiNH_2$[32,33] are shown in Figure 3. The N−H symmetric and asymmetric stretching vibrations of $LiNH_2$ occur at 3260 and 3315 cm^{-1}, respectively. Those bands in the Li−Al−N−H system shift to somewhat smaller wavenumbers by mechanical milling (N−H symmetric vibration, 3240 cm^{-1}; N−H asymmetric vibration, 3290 cm^{-1}). Li_2NH gives rise to the N−H stretching mode at 3180 cm^{-1}. The Li−Al−N−H system after H_2 desorption contains the stretch at 3190 cm^{-1} which is due to the presence of Li_2NH. The XRD peaks associated with Li_2NH, however, were not observed in the XRD curve of the Li−Al−N−H system. This can be understood by considering that Li_2NH in the Li−Al−N−H system has an amorphous structure. Thus, the H_2 desorption reaction of the Li−Al−N−H system can be expressed by eq 2

$$2Li_3AlH_6 + 4LiNH_2 \rightarrow Li_3AlN_2 + 2Li_2NH + 3LiH + Al + {}^{15}/_2H_2 \quad (2)$$

The experimental H_2 desorption capacity of the Li−Al−N−H system is 6.9 wt % and similar to that of the theoretical value of 7.6 wt % (based on eq 2). The dfference can be explained

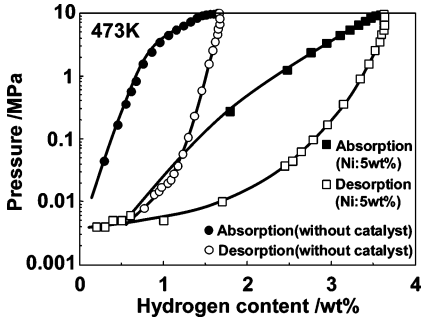

Figure 4. *P*−*C* isotherms for Li−Al−N−H systems.

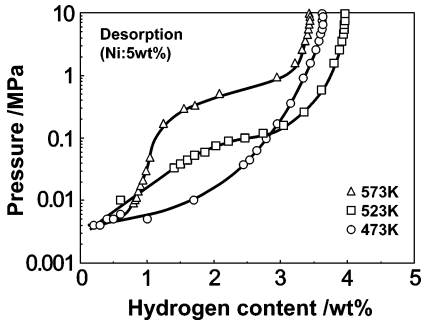

Figure 5. H_2 desorption isotherms for Li−Al−N−H system.

by H_2 desorption during ball-milling. The value for the standard enthalpy change upon hydrogen absorption (heat of formation) in eq 2 by the first-principles calculation is −23 kJ/mol H_2, while the calculated heat of formation from the data in the first-step reaction of eq 1 was −29 kJ/mol H_2.[30,34] The entropy change of hydrogen in the imide/amide reaction situation ($Li_2NH + H_2 \leftrightarrow LiNH_2 + LiH$) is roughly 120 J/mol H_2·K.[32] To reach a dissociation pressure of 1 bar with a heat of formation of −23 kJ/mol H_2, the temperature should be 192 K. Thus, the small absolute value of the heat of formation corresponds to high dissociation pressure. The high dissociation pressure may accelerate the dehydriding reaction of the Li−Al−N−H system at a lower temperature of around 370 K.

After H_2 desorption from the Li−Al−N−H system at 673 K for 15 h, the reaction rate of the Li−Al−N−H system at 473−573 K for both the absorption and desorption became slower. The *P*−*C* isotherms were obtained over a period of 40 h and for each data point equilibrated for approximately 1 h. Typical absorption and desorption isotherms for the Li−Al−N−H system at 473 K are presented in Figure 4. When H_2 is added into the tube containing the Li−Al−N−H system, H_2 is absorbed. The H_2 absorption capacity reaches a value of 1.6 wt % in the H_2 pressure of 10 MPa. The H_2 desorbed at the pressure of 0.004 MPa is 0.9 wt %. Figure 4 also shows the *P*−*C* isotherm of the Li−Al−N−H system with nano-Ni. The H_2 absorption and desorption capacities are 3.6 and 3.4 wt %, respectively. One can see that the capacities are remarkably increased by using the nano-Ni catalyst. The *PC* data in Figure 4 show very large hysteresis between a factor of about 10 to 100 in pressure. The desorption curves coincided each other when the reaction ratio was used as the *X*-axis. This behavior can be explained by assuming that the decomposition pressure has equilibrium state. Figure 5 shows H_2 desorption isotherms for the Li−Al−N−H system with nano-Ni. The Li−Al−N−H system with nano-Ni desorbs 3−4 wt % of hydrogen at 473−573 K in the pressure range 10−0.004 MPa. These values exceeded two times of the system without the catalyst (H_2 capacity, 1−2 wt %).

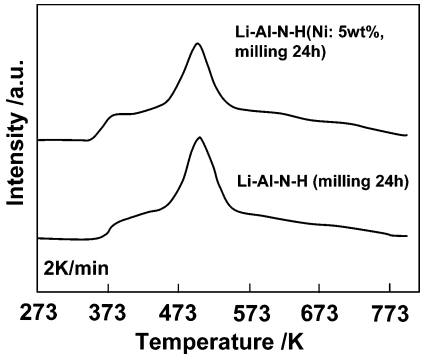

Figure 6. TPD spectra for Li−Al−N−H systems ($Li_3AlH_6/2LiNH_2$, $Li_3AlH_6/2LiNH_2$/Ni:5 wt %).

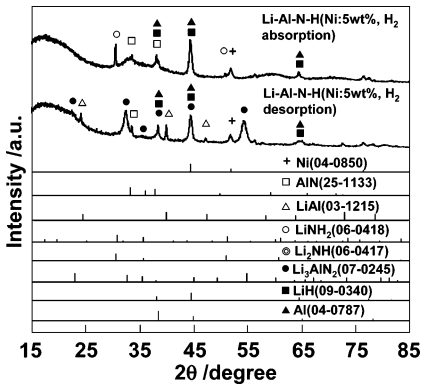

Figure 7. X-ray diffraction intensity curves for Li−Al−N−H system with nano-Ni together with the data of $LiNH_2$ (JCPDS file no. 06-0418), Li_2NH (JCPDS file no. 06-0417), Li_3AlN_2 (JCPDS file no. 07-0245), LiH (JCPDS file no. 09-0340), Al (JCPDS file no. 04-0787), Ni (JCPDS file no. 04-0850), AlN (JCPDS file no. 25-1133). and LiAl (JCPDS file no. 03-1215)

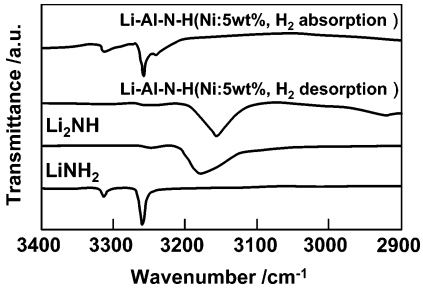

Figure 8. IR absorption spectra of Li−Al−N−H system with nano-Ni together with the data of Li_2NH[31,32] and $LiNH_2$.[31,32]

As shown in Figure 6, the initial H_2 desorption is observed from 350 K in the Li−Al−N−H system with nano-Ni. The temperature shifts to a lower value compared to that of the Li−Al−N−H system without the catalyst (370 K). The amount of H_2 desorbed from the Li−Al−N−H system with nano-Ni was 6.7 wt % and approximately independent of the catalyst content (5 wt %). These results indicate that the increased absorption and desorption capacities of the Li−Al−N−H system with nano-Ni by the *P*−*C* isotherms are responsible for the kinetic improvement by addition of the nano-Ni catalyst.

Figure 7 presents the XRD curves of the Li−Al−N−H system with nano-Ni before and after H_2 absorption together with the data of $LiNH_2$,[31] Li_2NH,[31] Li_3AlN_2,[31] LiH,[31] Al,[31] Ni,[31] AlN,[31] and LiAl.[31] The diffraction peaks of the Li−Al−N−H system with nano-Ni before H_2 absorption (after initial H_2 desorption) shows the presence of Li_3AlN_2, LiH, and Al, as was the case of the system without the catalyst. Figure 8 also shows that the Li−Al−N−H system with nano-Ni contains Ni,

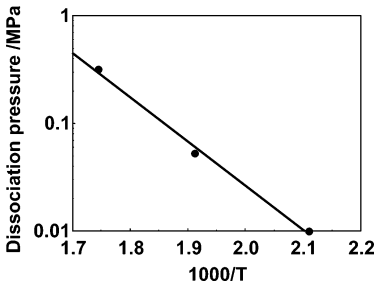

Figure 9. Van't Hoff plot for Li−Al−N−H system with nano-Ni.

AlN, and LiAl. After H_2 absorption, the XRD peaks of AlN, LiH, Al, Ni, and $LiNH_2$ or Li_2NH were observed. As the XRD curve of $LiNH_2$ phase is quite similar to that of Li_2NH phase, it is difficult to characterize the structure only from the XRD curves. The structure of the Li−Al−N−H system with nano-Ni was investigated by infrared spectroscopy. Figure 8 shows the infrared absorption spectra of the Li−Al−N−H system with nano-Ni, $LiNH_2$, and Li_2NH. The N−H symmetric and asymmetric stretching vibrations of $LiNH_2$ occur at 3260 and 3315 cm^{-1}, respectively.[32,33] Li_2NH gives rise to characteristic N−H stretching vibration at 3180 cm^{-1}.[32,33] We notice that the Li−Al−N−H system with nano-Ni before and after H_2 absorption contains Li_2NH and $LiNH_2$, respectively. Thus, the TPD spectra, the infrared absorption spectra and the XRD intensity curves show that the Li−Al−N−H system with nano-Ni before H_2 absorption is a mixture of Li_3AlN_2, Li_2NH, LiH, Al, LiAl, Ni, and AlN; while the Li−Al−N−H system with nano-Ni includes $LiNH_2$, LiH, Al, AlN, and Ni after H_2 absorption. Then, the H_2 absorption and desorption of the Li−Al−N−H system takes the following reaction path:

$$Li_3AlN_2 + 2Li_2NH + 3LiH + Al + 4H_2 \leftrightarrow 3LiNH_2 + 7LiH + Al + AlN \quad (3)$$

The reaction might be composed of two reactions given by $2Li_2NH + 2H_2 \leftrightarrow 2LiNH_2 + 2LiH$, which is the original imide/amide reaction described by Chen and co-workers,[16] and $Li_3AlN_2 + 2H_2 \leftrightarrow LiNH_2 + 2LiH + AlN$. Before writing those reactions, excess Al and LiH in eq 3 were canceled. H_2 of 4.2 wt % can be stored in this reaction. The H_2 absorbed of the Li−Al−N−H system with nano-Ni determined using the *P*−*C* isotherm was 3.6 wt % and a little lower than the theoretical value. The XRD curve and the infrared absorption spectrum also show that the Li−Al−N−H system with nano-Ni after initial H_2 desorption includes LiAl and Li_2NH. Then**,** the side reactions can be expressed as follows:

$$LiH + Al \rightarrow LiAl + {}^1/_2H_2 \quad (4)$$

$$Li_3AlH_6 + 2LiNH_2 \rightarrow Li_2NH + 3LiH + AlN + 3H_2 \quad (5)$$

Thermodynamic analysis was performed over the Li−Al−N−H system with nano-Ni. The Li−Al−N−H system obeys the van't Hoff equation, which relates the dissociation pressure to the absolute temperature.[4,32] We choose the pressure at the H_2 content of 1.7 wt % for calculation of the dissociation pressure. The values of the dissociation pressure obtained from the desorption isotherm at 473, 523, and 573 K were 0.010, 0.053, and 0.32 MPa, respectively (Figure 5). The van't Hoff plot is shown in Figure 9. The logarithm of the dissociation pressure versus the reciprocal of the absolute temperature yields a straight line. From the slope in Figure 9, the heat of formation is estimated to be −79 kJ/mol H_2. According to the first-principles calculations,[27,28] the heat of formation for eq 3 was estimated to be −70 kJ/mol H_2. The calculated heat of formation approximately agrees well with the experimental value for eq 3 (−79 kJ/mol H_2). This suggests that the desorption isotherms have equilibrium state. It is noted that the absolute value of the heat of formation is too large for practical applications.[4] Further studies are necessary to decrease the value.

4. Conclusions

Li_3AlH_6 and $LiNH_2$ were mechanically milled to form Li−Al−N−H systems. $LiNH_2$ destabilized Li_3AlH_6 during the dehydrogenation process of Li_3AlH_6. Hydrogen can be reversibly stored by the Li−Al−N−H system and the Li−Al−N−H system with nano-Ni. The H_2 absorption and desorption capacities of the Li−Al−N−H system with nano-Ni were 3−4 wt % and greater than twice that of the system without the catalyst. We found that the reversible capacity was remarkably improved using the nano-Ni catalyst.

Acknowledgment. This work is partially supported by the New Energy Industrial Technology Development Organization (NEDO), Development of Safe Utilization Technology, and an Infrastructure for Hydrogen Use (2004-2005).

References and Notes

(1) Schlapbach, L.; Züttel, A. *Nature (London)* **2001**, *414*, 353.
(2) Chahine, R.; Bose, T. K. *Int. J. Hydrogen Energy* **1994**, *19*, 161.
(3) Kojima, Y.; Suzuki, N. *Appl. Phys. Lett.* **2004**, *84*, 4113.
(4) Kojima, Y.; Kawai, Y.; Towata, S.; Matsunaga, T.; Shinozawa, T.; Kimbara, M. In *Symposium GG, Materials and Technology for Hydrogen Storage and Generation*; Nazri, G.-A., Ping, C., Young R. C., Nazri, M., Wang, J., Eds.; *Mater. Res. Soc. Symp. Proc.* **2005**, *884E*, GG6.5. Kojima, Y.; Kawai, Y.; Towata, S.; Matsunaga, T.; Shinozawa, T.; Kimbara, M. *J. Alloys Compd.* In press.
(5) Amendola, S. C.; Sharp-Goldman, S. L.; Janjua, M. S.; Kelly, M. T.; Petillo, P. J.; Binder, M. *J. Power Sources* **2000**, *85*, 186.
(6) Kojima, Y.; Suzuki, K.; Fukumoto, K.; Sasaki, M.; Yamamoto, T.; Kawai, Y.; Hayashi, H. *Int. J. Hydrogen Energy* **2002**, *27*, 1029.
(7) Li, Z. P.; Liu, B. H.; Arai, K.; Morigazaki, N.; Suda, S. *J. Alloys Compd.* **2003**, *356*−*357*, 469.
(8) Züttel, A.; Wenger, P.; Rentsch, S.; Sudan, P.; Mauron, Ph.; Emmenegger, Ch. *J. Power Sources* **2003**, *118*, 1.
(9) Kojima, Y.; Kawai, Y.; Kimbara, M.; Nakanishi, H.; Matsumoto, S. *Int. J. Hydrogen Energy* **2004**, *29*, 1213.
(10) Bogdanovič, B.; Schwickardi, M. *J. Alloys Compd.* **1997**, *253*−*254*, 1.
(11) Fichtner, M.; Engel, J.; Fuhr, O.; Kircher, O.; Rubner, O. *Mater. Sci. Eng., B* **2004**, *108*, 42.
(12) Kojima, Y.; Suzuki, K.; Kawai, Y. *J. Mater. Sci. Lett.* **2004**, *39*, 2227.
(13) Kojima, Y.; Kawai, Y.; Haga, T. In *Symposium N Materials for Hydrogen Storage*; Vogt, T., Stumpf, R., Heben, M., Robertson, I., Eds.; *Mater. Res. Soc. Symp. Proc.* **2004**, *837*, N3.5. Kojima, Y.; Kawai, Y.; Haga, T. *J. Alloys Compd.* In press.
(14) Hanada, N.; Ichikawa, T.; Fujii, H. *J. Phys. Chem. B* **2005**, *109*, 7188.
(15) Newson, E.; Haueter, Th.; Hottinger, P.; Von, Roth, F.; Scherer, G. W. H.; Schucan, Th. H. *Int. J. Hydrogen Energy* **1998**, *23*, 905.
(16) Chen, P.; Xiong, Z.; Luo, J.; Lin, J.; Tan, K. L. *Nature (London)* **2002**, *420*, 302.
(17) Nakamori, Y.; Orimo, S. *J. Alloys Compd.* **2004**, *370*, 271.
(18) Leng, H. Y.; Ichikawa, T.; Hino, S.; Hanada, N.; Isobe, S.; Fujii, H. *J. Phys. Chem. B* **2004**, *108*, 8763.
(19) Luo, W. *J. Alloys Compd.* **2004**, *381*, 284.
(20) Orimo, S.; Nakamori, Y.; Kitahara, G.; Miwa, K.; Ohba, N.; Noritake, T.; Towata, S. *Appl. Phys. A* **2004**, *79*, 1765.
(21) Xiong, Z.; Wu, G.; Hu, J.; Chen, P. *Adv. Mater.* **2004**, *16*, 1522.
(22) Nakamori, Y.; Ninomiya, A.; Kitahara, G.; Aoki, M.; Noritake, T.; Miwa, K.; Kojima, Y.; Orimo, S. *J. Power Sources* In press.
(23) Xiong, Z.; Wu, G.; Hu, J.; Chen, P. *ABSTRACTS Symposium P Materials for Rechargeable Batteries, Hydrogen Storage and Fuel Cells*; 3rd International Conference on Materials for Advanced Technologies (ICMAT 2005) and 9th International Conference on Advanced Materials (ICAM 2005), July 3−8, 2005, Singapore; PB-7-OR9, p 20.
(24) Lu, J.; Fang, Z. Z. *J. Phys. Chem. B* **2005**, *109*, 20830.

(25) Chen, J.; Kuriyama, N.; Xu, Q.; Takeshita, H, T.; Sakai, T. *J. Phys. Chem. B* **2001**, *105*, 11214.

(26) Balema, V. P.; Pecharsky, V. K.; Dennis, K. W. *J. Alloys Compd.* **2000**, *313*, 69.

(27) Miwa, K.; Fukumoto, A. *Phys. Rev. B* **2002**, *65*, 155114.

(28) Miwa, K.; Ohba, N.; Towata, S.; Nakamori, Y.; Orimo, S. *Phys. Rev. B* **2004**, *69*, 245120.

(29) Ichikawa T.; Isobe, S.; Hanada, N.; Fujii, H. *J. Alloys. Compd.* **2004**, *365*, 271.

(30) Dymova, T. N.; Aleksandrov, D. P.; Konoplev, V. N.; Silina, T. A.; Sizareva, A. S. *Russ. J. Coord. Chem.* **1994**, *20*, 263.

(31) Powder Diffraction File; Publication Manager, Kahmer, T. M.; Editor-in-Chief, McClune, W. F.; Editor of Calculated Patterns, Kabekkodu, S. N.; Staff Scientist, Clark, H. E.; Database Programmer, Bosnic, V.; International Centre for Diffraction Data (JCPDS), Pennsylvania, 2004.

(32) Kojima, Y.; Kawai, Y. *J. Alloys Compd.* **2005**, *395*, 236.

(33) Kojima, Y.; Kawai, Y. *Chem. Commun.* **2004**, *19*, 2210.

(34) Løvvik, O. M.; Opalka, S. M.; Brinks, H. W.; Hauback, B. C. *Phys. Rev. B* **2004**, *69*, 134117.